IEEE Access
Multidisciplinary | Rapid Review | Open Access Journal

Received 1 May 2023, accepted 15 May 2023, date of publication 17 May 2023, date of current version 30 May 2023.

Digital Object Identifier 10.1109/ACCESS.2023.3277390

APPLIED RESEARCH

Design, Analysis and Fabrication of an Inside-Grooved Slotted Waveguide Array Antenna for HPM Applications

ASIF MEHMOOD KHAN, MUHAMMAD M. AHMED, (Senior Member, IEEE), UMAIR RAFIQUE, (Member, IEEE), AND SULEMAN KHAN
Department of Electrical Engineering, Capital University of Science and Technology, Islamabad 44000, Pakistan
Corresponding author: Muhammad M. Ahmed (mansoor@cust.edu.pk)

ABSTRACT In this paper, a slotted waveguide array antenna (SWAA) is designed for S-band high-power microwave (HPM) applications. The single element of the array consists of ten Gaussian distributed slots on the broad wall of the waveguide, integrated with inside grooves. The 4-element SWAA configuration is designed to achieve a relatively high gain (24.6 dB) along with highly isolated (−24 dB) radiating elements. The gain enhancement and mutual coupling (MC) reduction is achieved by optimizing inside-grooved regions. An efficient 1×4 power divider (PD) of identical phase and magnitude (−6 dB) at its output ports, is designed to feed the array elements. The radiation performance of SWAA is further improved by developing a dielectric radome. The proposed design is compact having dimensions $8.46\lambda_0 \times 4.3\lambda_0 \times 1.47\lambda_0$, and offers return loss (RL) better than −25 dB with side lobe level (SLL) of −15 dB and −20 dB in E and H-plane, respectively. The designed array has 95.78% antenna efficiency over 3.8% measured bandwidth with 63% aperture efficiency. It has been demonstrated that the developed system, because of effective suppression of unwanted surface current, provides ±22° beam scanning without causing a significant reduction in its gain. The technique, without adding any complexity in the system, offered a 7% improvement in the gain when compared with a similar design.

INDEX TERMS Slotted waveguide, high power microwave, array antenna, beam scanning, dielectric radome, power divider.

NOMENCLATURE

SWA	Slotted waveguide antenna.
SWAA	Slotted waveguide array antenna.
HPM	High power microwave.
PD	Power divider.
SLL	Side lobe level.
SF_6	Sulphur hexafluoride.
N_2	Nitrogen.
HDPE	High density polyethylene.
RADAR	Radio detection and ranging.
GW	Giga Watts.
RL	Return loss.
MC	Mutual coupling.
P_A	Power at aperture.
P_{in}	Input power.
P_R	Power at radome.
f_0	Center frequency.
λ_g	Guided wavelength.
λ_0	Center frequency wavelength
S_{ij}	Scattering parameters.
CST	Computer simulation technology.
CCTV	Closed circuit TV.
EM	Electromagnetic.
MWS	Microwave studio.
UAV	Unmanned area vehicle.
VNA	Vector network analyzer.
E	Electric field.
H	Magnetic field.
E_{ant}	Electric field at antenna.

The associate editor coordinating the review of this manuscript and approving it for publication was Tutku Karacolak.

E_{AB} Air breakdown field.
E_{GB} Waveguide breakdown field.

I. INTRODUCTION

In the past few years, high-power microwave (HPM) technology become popular for both civilian and military applications. There are many HPM devices and systems in the world, like active denial systems which are used as a non-lethal weapons to fortify a defence system. Electronic devices and circuits can be damaged/disrupted by HPM weapons since many commercial applications such as WiFi modules, wireless CCTV cameras, UAVs and Bluetooth devices typically operate in S-band. Maximum damage occurs when the frequency of the HPM device is the same as that of the target device. Additionally, due to the relatively large size of the transmit antenna, a gigawatt (GW) HPM signal can be achieved in S-band without breakdown [1], [2].

In an HPM system, the transmit antenna has a very crucial role [3], [4], [5]. It is an established fact that the efficiency of an entire HPM system depends upon its radiating antenna. The antenna elements handle HPM pulses and transmit them in the air without attaining breakdown. The most popular antenna in an HPM system is the horn antenna, which is widely employed due to its simpler design. However, it cannot provide an efficient beam directivity and its beam scanning capability is also limited [6]. A controlled beam scanning with high power handling capacity and low SLL are considered crucial parameters for an HPM system. A practical realization of such a system is a challenging task, because of the design complexity and mechanical movement of the antenna. Furthermore, the movement of a large mechanical structure defining an HPM system causes large power consumption in addition to an associated inertia which may generate a delay to hit the target [6]. To overcome these limitations, different HPM antenna array systems have been proposed in [7], [8], [9], [10], and [11]. But one of the major restrictions in these designs is large SLL both in azimuth and elevation planes.

A 4-element grooved structure based SWA configuration is reported in [9]. In this design, unwanted coupling between the elements of antenna was addressed by employing grooves in between the elements of array. This technology restrained the mutual coupling (MC) of the slots. A significant improvement in beam scanning was also achieved by integrating the choked region without making any compromise on 3 dB gain.

The groove structures in the slotted array configuration is used for a dual purpose i.e., MC reduction and gain enhancement. The MC among the array elements degrades the beam scanning ability of the system and causes backward power flow i.e., towards the source. These are the critical issues in the design of a phased array antenna with large beam steering requirements [7]. The unwanted MC among the array elements is overcome by using different techniques including but not limited to inter-element spacing, metal wall integration, frequency selective surfaces, metamaterial structures, and grooved regions [12], [13], [14]. Finding an optimum slot spacing eliminates nulls and grating lobes, and is considered a challenging task in the design of an HPM phased array antenna. The transmission and beaming effects of SWAs can be enhanced by incorporating grooved structures near the slots, which result in improved radiation characteristics by reducing MC. These customized regions help in suppressing the surface wave propagation as observed in choke structures. The re-distribution of electromagnetic waves in the slotted regions produces high surface currents and MC, which can be suppressed effectively by incorporating a grooved structure appropriately [15], [16].

A 10-slot based rectangular SWA configuration integrated with non-periodic grooves and dielectric radome is reported in [13]. The integration of one-dimensional corrugated grooves re-radiate the EM waves to the targeted direction by properly optimizing the period, width, position, and depth. This antenna configuration offered a gain of 20.1 dBi with significant suppression in the back-lobe of the antenna. Moreover, dielectric radome was also deployed to maintain the radiation characteristics without compromising the performance parameters. A beam steerable SWA array is presented in [12]. The C-shape slots were cut on the narrow wall of the waveguide to feed the spiral helical unit elements to achieve circular polarized waveform. A gain of 26.3 dBi was achieved with wide angle beam scanning capability, whereas, a maximum of 2 dBi gain degradation was reported during the beam scanning [10].

In [17], the authors proposed a leaky wave antenna array to improve gain and impedance matching. The array configuration was properly coupled with a 48-way power divider for an efficient far-field radiation pattern. An optimized SWA integrated grooved structure can be employed to avert impedance matching issues, especially in the presence of a secondary source. The grooved structure in an array formation suppresses the undesirable surface currents which as a result improves isolation. Properly decoupled array elements provide efficient wide angle beam scanning capabilities with minimum grating lobes emergence.

In SWA, high power handling might require that the system should be operated in vacuum or in the presence of a suitable gaseous environment such as SF_6 or N_2 to improve E-field breakdown. For this purpose, SWA should be enclosed with a suitable structure that should help in maintaining the high amplitude radiation characteristics of SWA [18], [19], [20]. Such a structure could be a radome provided it would not disturb the radiation characteristics of the array. If such a radome is appropriately designed, it would also contribute to immune the system from its vicinity. Therefore, a proper design of the radome is required to reduce the impact on high magnitude radiation parameters and to improve the performance of the HPM system. Moreover, proper analysis of radome structure along with antenna structure design is required to improve the radiation performance of the system in totality.

TABLE 1. Target design parameters of slotted waveguide array antenna (SWAA) for high power microwave applications.

Design Variables	Target Values
Operating frequency	3 GHz
Directivity	Higher than 25 dBi
Return loss	Less than −20 dB
Mutual coupling	Less than −20 dB
SLL in H-plane	Less than −20 dB
Number of slots	10
Number of elements	04

In this article, an efficient SWA has been designed, fabricated and tested for HPM applications. To achieve HPM capabilities, rectangular waveguide loaded with optimally designed grooves along with high density polyethylene (HDPE) radome have been investigated. It has been demonstrated that the integration of grooves in an array configuration reduces MC, improves radiation patterns and provides a wide-range beam scanning ability. Moreover, a dielectric radome is designed to allow the HPM functionalities of the SWA aperture under a specific ambient. The organization of the remaining parts of the paper is that Section II briefly outlines the design of the grooved SWAA system whilst Section III gives details pertaining to SWAA fabrication and measurements. Finally, the conclusions drawn from this research are presented in Section IV.

II. INSIDE-GROOVED SLOTTED WAVEGUIDE ARRAY ANTENNA

The purpose of this section is to design and analyze SWAA with grooved structures. To assess the role of a radome in achieving controlled radiation ambient at the aperture of SWAA, and to develop a 1×4 waveguide based PD to realize a complete system. Also, a comparison is made between the conventional and proposed design of SWAA by considering directivity, SLL, MC and beam steering. The target variables to realize a good SWAA system, have been identified and listed in Table 1.

A. ONE TO FOUR (1×4) POWER DIVIDER (PD)

Power dividers are widely employed in communication systems and RADAR with the purpose to feed elements of an array antenna. The main requirement for designing a PD is that it should have low insertion loss, equal power division, same output phase, and the ability to handle high power such as GW. Due to high power handling requirements, waveguide based PD is employed to feed an antenna array system meant for HPM applications.

As listed in Table 1, the required 1×4 PD was designed using standard WR-284 waveguide dimensions. The main designing constraints of the target PD were, the amplitudes

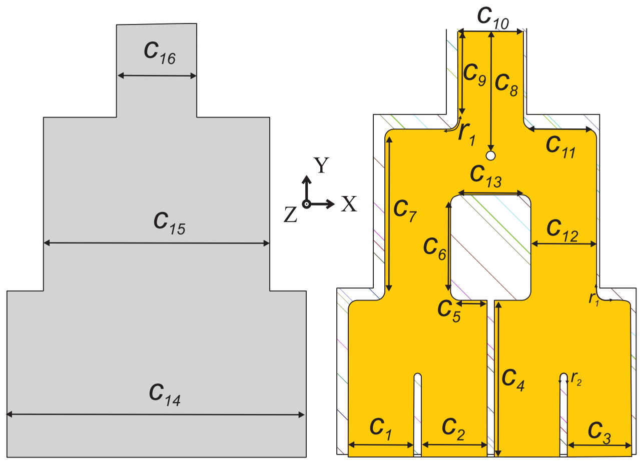

FIGURE 1. Top and cut-view of waveguide based 1 × 4 power divider (PD) to feed slotted waveguide array antenna (SWAA).

TABLE 2. Various dimensions (mm) of a 1 × 4 waveguide based power divider (PD) as shown in Fig. 1.

Variable	C_1	C_2	C_3	C_4	C_5	C_6
Value	72.14	72.14	72.14	180.14	30.07	95.86
Variable	C_7	C_8	C_9	C_{10}	C_{11}	C_{12}
Value	168	137	100.92	72.14	60.14	72.14
Variable	C_{13}	C_{14}	C_{15}	C_{16}	r_1	r_2
Value	68.14	328.56	248.42	88.14	10	4

and phases of signals at its output ports relative to the signal given at its input. To ensure equal output amplitude, which in this case was −6 dB, the length of waveguides was chosen equal to the wavelength of central frequency (λ_0). Under this condition, the output phases will also be the same, however, a possible mismatch between input and output ports due to non-equal prorogation delay is controlled by placing a septum (small cylindrical rod) at a particular position. The simulation has been performed in CST microwave studio (MWS). The top and cut-view of 1×4 PD are shown in Fig. 1, whereas, the dimensions of the proposed design are explained in Table 2.

The magnitude of reflection parameter S_{11} along with various transmission parameters ($S_{12}, S_{13}, S_{14}, S_{15}$) are shown in Fig. 2. The plots of Fig. 2 show $S_{11} = -40$ dB with an output amplitude of −6 dB from all output ports of the PD. This confirms that, from input to output, the power has been divided in equal parts. For efficient beam forming the signals at the output ports of the PD should be in phase. Fig. 3 shows the output phases of 1×4 PD, which are almost overlapping and hence, the phases are synchronized. The position of the septum was optimized by doing parametric analysis as shown in Figure 4(a). The graph shows that for $C_8 = 137$ mm, there were minimal reflections and maximum transmission from input to output, thus ensuring synchronized output signals with equal power division at the output ports of the

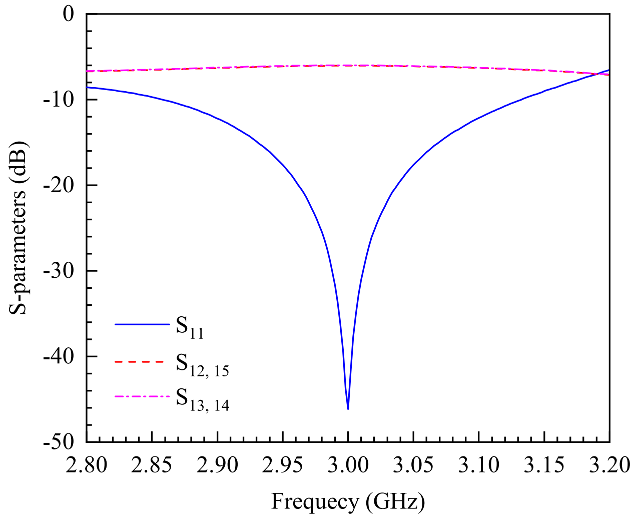

FIGURE 2. Reflection (S_{11}) along with transmission parameters ($S_{12}, S_{13}, S_{14}, S_{15}$) of a 1 × 4 power divider.

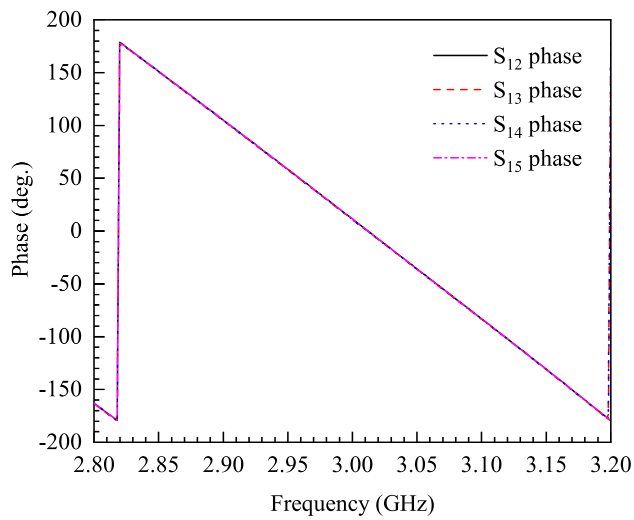

FIGURE 3. Output phases of a 1 × 4 power divider.

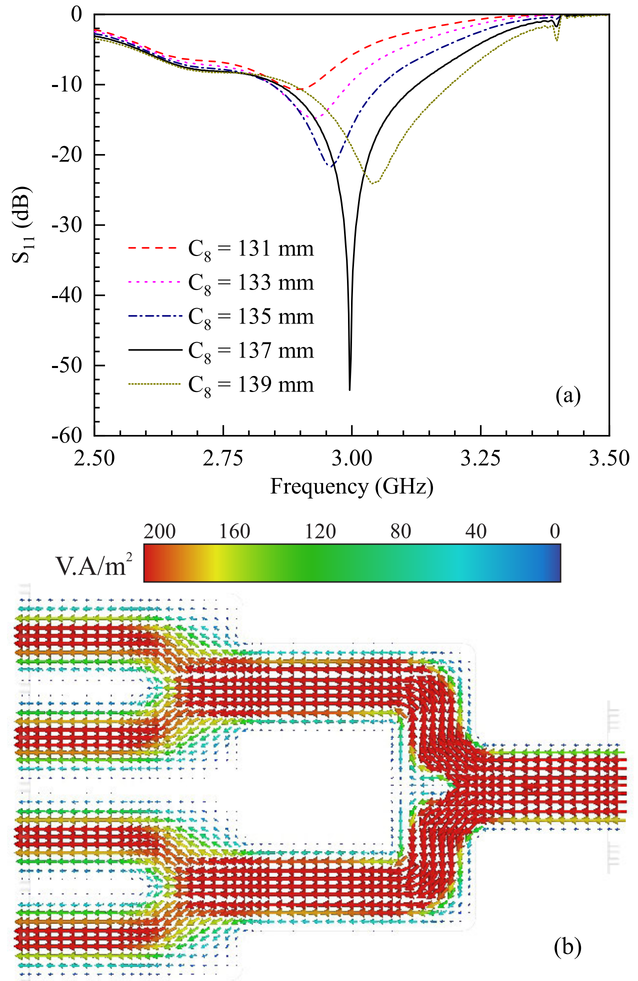

FIGURE 4. Exhibits (a) optimization of septum position for 1 × 4 power divider (b) simulated power flow for C_8 = 137 mm.

PD [21], [22], [23]. Additionally, the power flow pattern of the designed PD is illustrated in Fig. 4(b). It can be seen from the figure that the power is equally distributed from input to output, which exhibits a uniform power flow across each port of the PD.

B. DESIGN OF INSIDE-GROOVED BASED SLOTTED WAVEGUIDE ARRAY ANTENNA (SWAA)

The proposed slotted waveguide array antenna consists of 4 elements and 10 slots. Each element is separated by an inside groove to minimize MC and to increase the directivity of SWAA. In this section, first the single element of grooved SWAA will be discussed followed by the complete design of SWAA along with its simulated results.

1) SINGLE ELEMENT GROOVED SWA

In this section, the single element inside grooved-based slotted waveguide antenna has been analyzed. The detailed design of grooved structure in SWA and its associated parameters including Gaussian profile, its importance in surface current suppression is studied by our group and presented in [13] wherein, it has been established that the use of a Gaussian shaped dielectric radome improves the power handling capability as well as the directivity of SWA.

A standard WR284 ($a = 72.14$ mm, $b = 34.04$ mm) waveguide is used to design and simulate the single grooved-based slotted waveguide antenna for 3 GHz frequency as shown in Fig. 5. The depth of the groove on wall of the waveguide is about 0.23 λ_0 with 0.04 λ_0 and 8.17 λ_0 as its width and length, respectively. The grooved-based technique results in surface current suppression on the aperture of the antenna. The Gaussian profile slots distribution has been applied to achieve the desired SLL of at least −20 dB. The coefficient and the corresponding position of 10 slots are given in

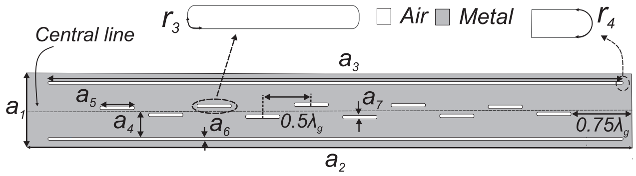

FIGURE 5. Single element of a grooved slotted waveguide antenna (SWA) ($a_1 = 88.14$ mm, $a_2 = 890$ mm, $a_3 = 817$ mm, $a_4 = 40.07$ mm, $a_5 = 49.42$ mm, $a_6 = 4$ mm, $a_7 = 10$ mm, $\lambda_g = 138.5$, $r_3 = 5$ mm, $r_4 = 2$ mm).

TABLE 3. Gaussian distribution coefficients and slot displacement from the central line of SWA.

Slot	Gaussian Coefficients	Slots Displacement (mm)
1	1.000	4.5936
2	1.4474	5.5432
3	2.3194	8.3332
4	3.1914	8.9273
5	3.6388	8.9273
6	3.6388	8.3332
7	3.1914	5.5432
8	2.3194	7.0599
9	1.4474	5.5432
10	1.000	4.5936

Table 3 [13]. The slots have round edges to avoid electric field concentration and local scattering. The guided wavelength for WR284 waveguide at $f_0 = 3$ GHz is 138.5 mm, which is calculated using Eq. 1:

$$\lambda_g = \frac{\lambda_0}{\sqrt{1-\left(\lambda_0/\lambda_{cutoff}\right)^2}} \tag{1}$$

2) GROOVED SLOTTED WAVEGUIDE ARRAY ANTENNA (SWAA)

The SWA elements are placed with a gap of less than half of the operating wavelength, to avoid grating lobes in the radiation pattern. The prime purpose of the grooved structure is to constraint surface current distribution within the respective surface area of the array element with the aim to improve directivity and reduce MC between the adjacent elements. The design, therefore, has 4 radiating elements with 7 grooves in total. The side and top view of the 4 elements array antenna used for CST simulation, is shown in Fig. 6.

The RL plot of SWAA is shown in Fig. 7. It can be seen that at the target frequency i.e., 3 GHz, the antenna gives minimum reflections; validating the perceived design. It can also be seen from the plots of the figure that the S_{22} and S_{33} values, which represent the middle two elements, are although within well allowed margin yet they are relatively poor. It is further observed that the magnitude of S_{22} and S_{33}, as a function of frequency, is identical and their associated central frequency is slightly shifted relative to S_{11} and S_{44}.

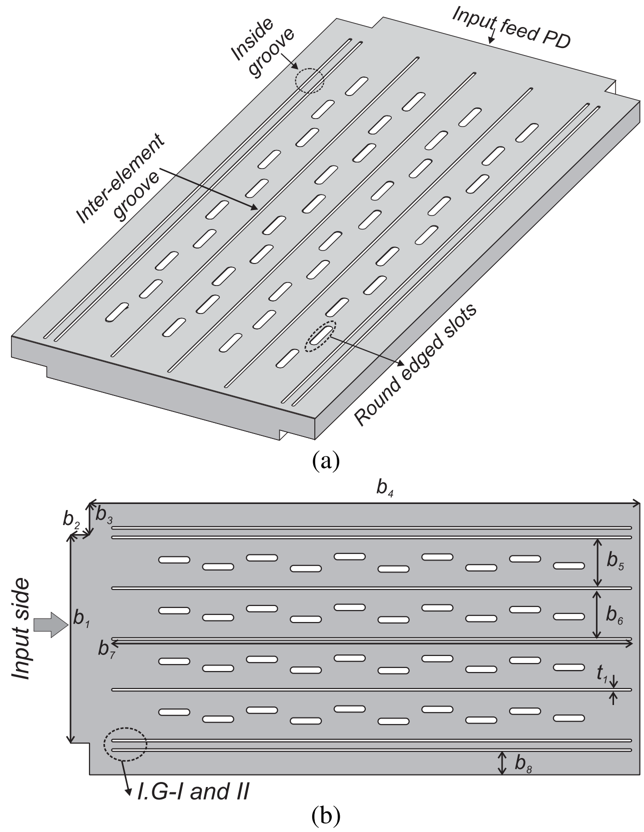

FIGURE 6. (a) 3D view and (b) top view of grooved slotted waveguide array antenna (SWAA) for high power microwave systems. The dimensions of various variables shown in the figure are: depth of I.G-I = 23 mm, I.G-II = 20.8 mm, $b_1 = 328$ mm, $b_2 = 30$ mm, $b_3 = 50$ mm, $b_4 = 869$ mm, $b_{5,6} = 76.14$ mm, $b_7 = 817$ mm, $b_8 = 37$ mm, $t_1 = 4$ mm.

A plausible explanation of this minor variation between two sets of reading, i.e. [S_{22}, S_{33}] and [S_{11}, S_{44}], could be associated with the variation in their respective structure. Array elements at the shoulder of the antenna have two side grooves, as evident from Fig. 6, whereas, two middle elements of the array contain one groove on each side. Hence, there are two sets of responses that are identical to each other, i.e S_{22} is the same as S_{33} likewise S_{11} and S_{44}. Since majority of the input power is transmitted by the antenna as RL of the antenna is less than −30 dB (Fig. 7), therefore, the magnitude of residual power in the band of interest is supposed to be very low and hence, its contribution to reflect the propagating signal is assumed to be negligible.

Fig. 8 shows MC values between the elements of SWAA which around the frequency of interest is below −22.4 dB. These values of MC are realized by appropriately introducing the groove structure inside the wall of the waveguide. It can be seen from the plot of Fig. 8 that MC between elements 2 and 3 is relatively higher compared to element 1 and 4. However, the attained values are still reasonably well within the allowed margin of targeted design values. The associated reason of this variation could be the same as that offered in the case of reflection coefficients

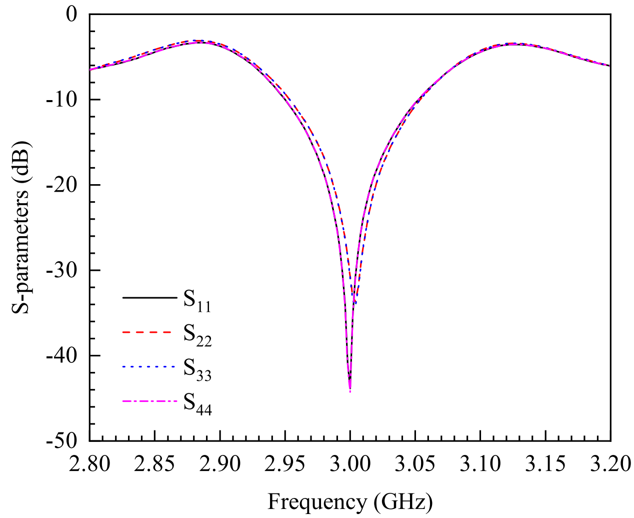

FIGURE 7. Reflection (S_{11}) plot of slotted waveguide array antenna (SWAA).

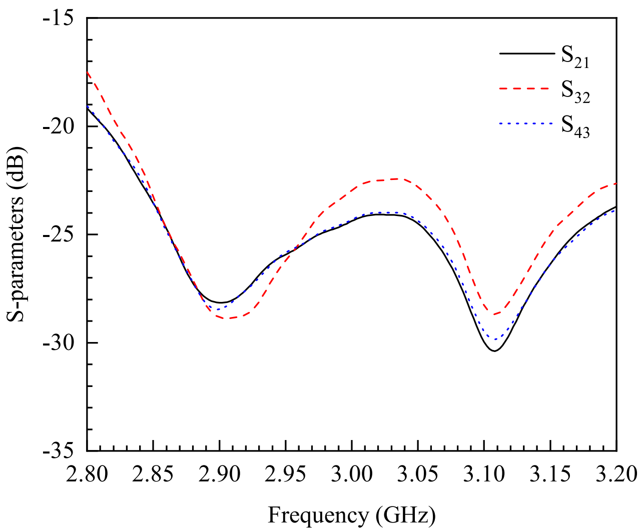

FIGURE 8. Mutual coupling (MC) between different elements of slotted waveguide array antenna (SWAA).

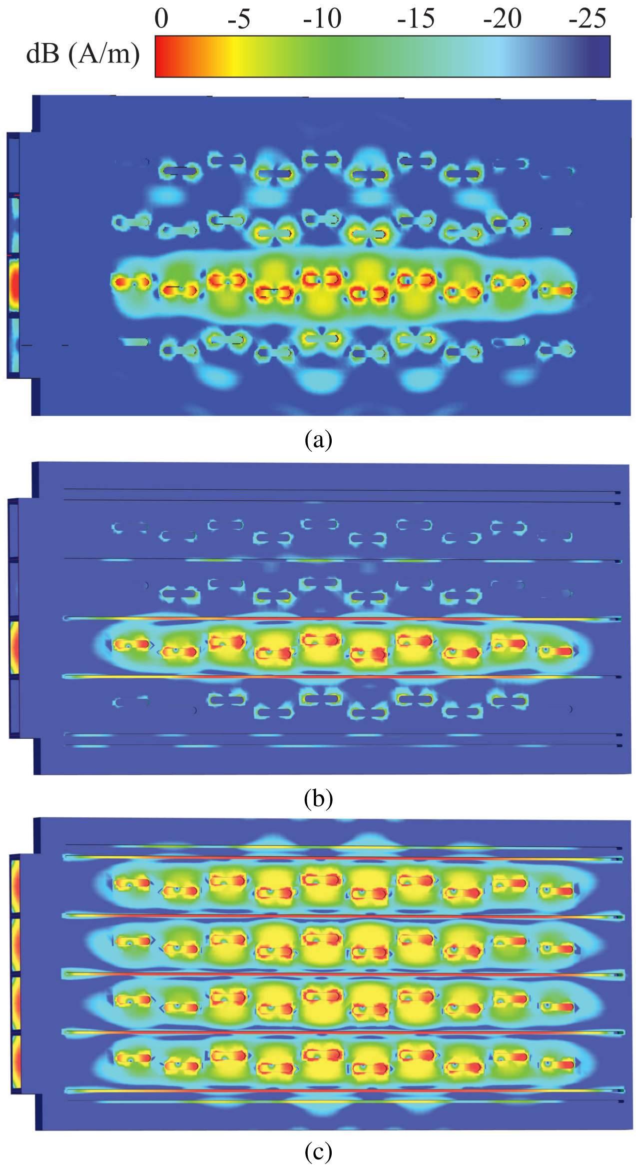

FIGURE 9. Surface current distribution pattern, in a four elements slotted waveguide array antenna, when only 3rd element of the array is excited (a) without (b) with groove structure and (c) when all elements are excited.

variation earlier. It is pertinent to mention here that reduction in MC is considered an essential component of an array antenna design to achieve high directivity and efficient beam forming. It has been noticed that the introduction of a groove in SWAA structure reduces the propagation of surface current between the elements as shown in Fig. 9. To compare the conventional SWAA with the proposed groove-based SWAA, the surface current propagation between the two designs has been simulated by exciting element 3 of both the design and shown in Fig. 9(a,b). It can be seen that there is a significant surface current spread in conventional SWAA [Fig. 9(a)], especially at the center of the waveguide, which eventually increases MC between the elements. The same is restricted to the respective element in the case of grooved geometry as evident in Fig. 9(b). To observe the holistic view of surface current confinement, all four inputs of the grooved structure have been excited simultaneously and the effect is shown in Fig. 9(c). This figure clearly demonstrates that the groove structure constraints surface current reasonably well in their respective regions and resultantly, there would be a reduction in MC between array elements. The additional groove is added to further reduce surface current propagation at the edges of the antenna array to prevent radiation pattern deterioration.

To have a comparative analysis of the two designs, a) the un-grooved design referred to as the conventional design, and the grooved one, the MC profile of the designed antenna

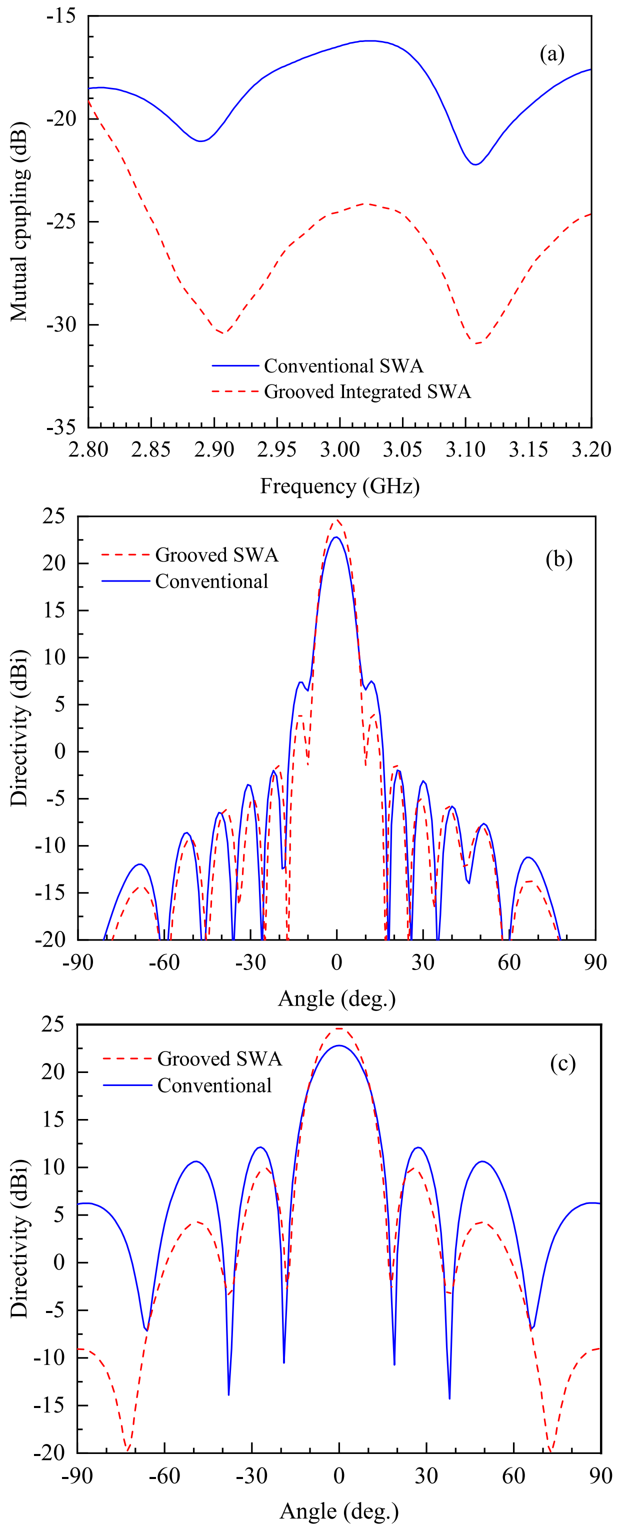

FIGURE 10. **(a) Mutual coupling, (b) H-plane and (c) E-plane radiation patterns of conventional vs grooved slotted waveguide array antenna (SWAA).**

element 3 and 4, is shown in Fig. 10(a). It can be seen from the plot that in the grooved structure, the MC is less than −22 dB whereas, the conventional structure offers −16 dB at

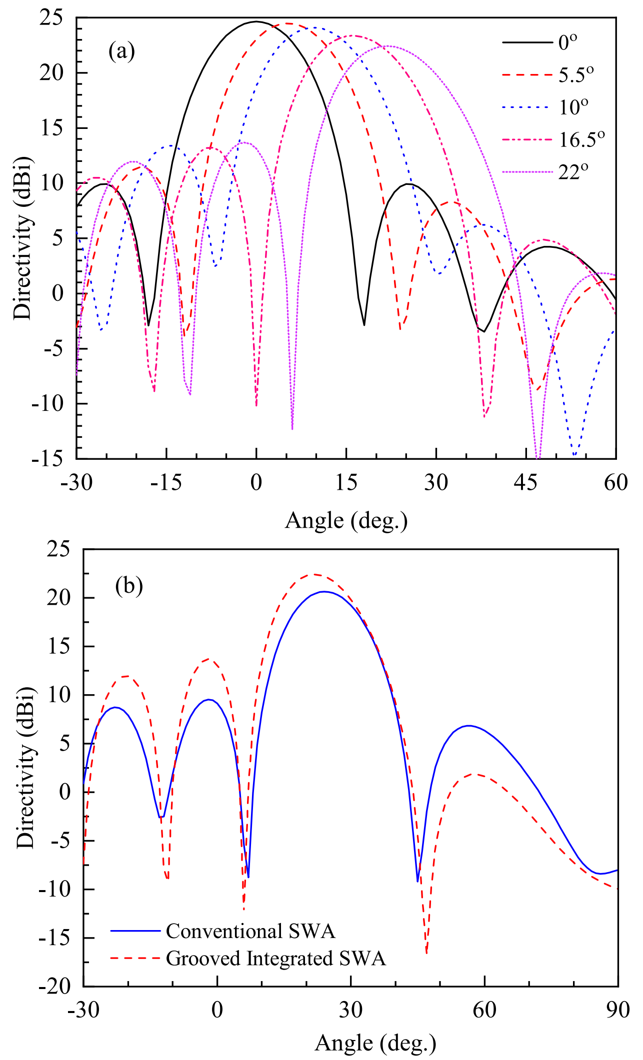

FIGURE 11. **(a) Beam steering capability of a four element slotted waveguide array antenna (SWAA) system and (b) represents directivity of conventional (without grooved) vs proposed (with grooved) slotted waveguide array antenna (SWAA).**

the frequency of interest. This is 37% higher than the grooved design. Such a high value of MC could eventually lead to deteriorated directivity of the system.

The H and E-plane radiation patterns of conventional and grooved SWAA are shown in Fig. 10(b,c). It can be seen that the H-plane radiation pattern of conventional SWAA has 8.8% less directivity than the grooved SWAA. Additionally, the main lobe profile is affected by the two upper lobes appearing in the shoulders of the main lobe. As shown in Fig. 10(c), the E-plane radiation pattern for the conventional SWAA also has a high value of grating lobes compared to the proposed design. In the nutshell, it can be said that in the given physical SWA structure, the proposed design, without adding any additional components, could enhance the operational performance of SWA, simply by manoeuvring the slot design and its surroundings.

TABLE 4. Comparison of performance parameters of slotted waveguide array antenna (C-SWAA) vs the proposed grooved slotted waveguide array antenna (G-SWAA).

Antenna Type	RL (dB)	MC (dB)	Dir. at 0 ° (dBi)	Dir. at 22 ° (dBi)
C-SWAA	−28	−16.5	22.6	20.46
G-SWAA	−30	−25	24.6	22.54
Ref. [9]	−25	–	22.91	20.5

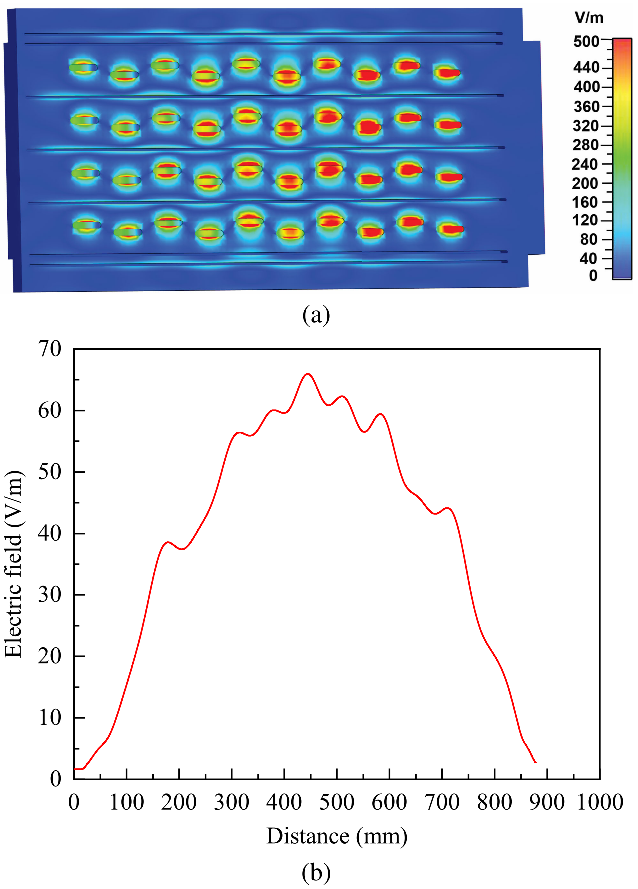

FIGURE 12. Electric field variation (a) at aperture and (b) at radome of a 4-element array antenna when excited with 0.5 W input signal.

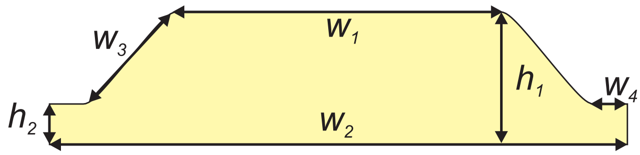

FIGURE 13. Dielectric radome for grooved slotted waveguide array antenna (W_1 = 240 mm, W_2 = 428 mm, W_3 = 68 mm, W_4 = 25 mm, h_1 = 98 mm, h_2 = 30 mm).

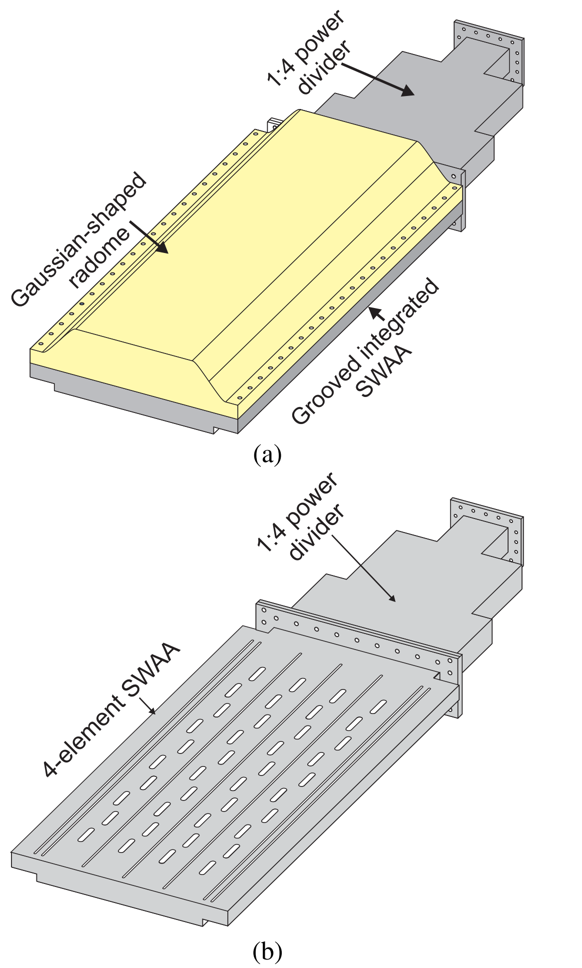

FIGURE 14. Complete physical illustration of a slotted waveguide array antenna (SWAA) (a) with and (b) without dielectric radome.

The beam steering capability of the proposed SWAA design has also been analyzed and shown in Fig. 11(a). It can be seen that the main lobe direction changes its position from 0° to 22° with minimal grating lobes. The variation in gain because of beam steering for the two designs under discussion is shown in Fig. 11(b). It can be seen from the plot that at the given beam steering, the directivity of proposed SWAA is better than the conventional SWAA by 2.1 dBi with low magnitude of grating lobes as well. This shows that the proposed design offers 13% improved performance than the conventional design. The performance summary of the two designs has been tabulated and presented in Table 4. In [9], Yong et.al. presented a 4-element waveguide-based array antenna for L-band high power applications. The reported values of Yong et.al. design are also listed in Table 4. It can be seen from the data that the proposed design is 16.6% better in RL relative to Yong's design, 7.4% at zero angle directivity and it offers 9.7% improved directivity at 22°.

To calculate power handling capacity; the electric field distribution on the aperture of SWAA is simulated and shown in Fig. 12. The maximum electric field intensity on the antenna aperture is 500 V/m (Fig. 12a) when the structure is excited with an input power P_{in} = 0.5 W. This leads to power

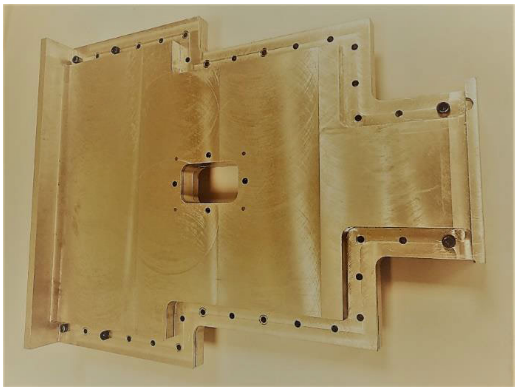

(a)

(b)

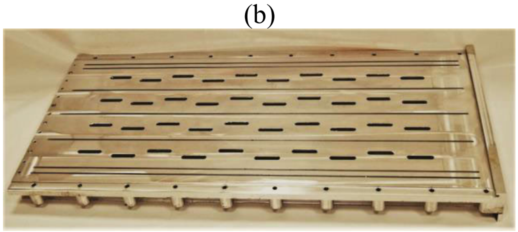

(c)

FIGURE 15. Components of fabricated slotted waveguide array antenna (SWAA): (a) top view of a 1:4 power divider, (b) crossectional view of the power divider and (c) 4-element slotted waveguide array with 7 inside horizontal groove.

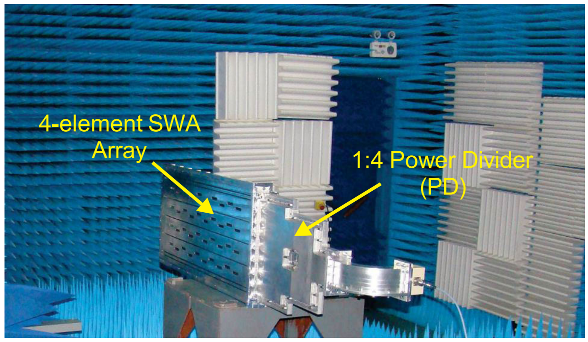

(a)

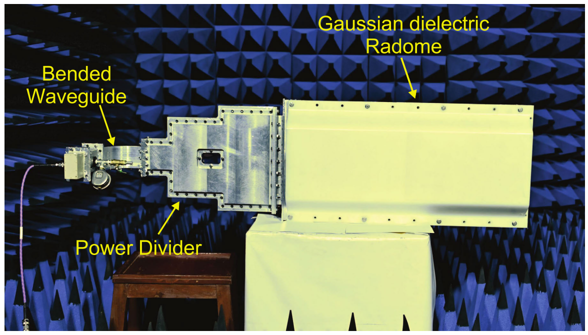

(b)

FIGURE 16. Pictorial view of an assembled slotted waveguide array antenna (a) without radome (b) with radome in an anechoic chamber for measurements.

handling capacity at the aperture, P_A, as

$$P_A = \frac{P_{in}(E_{GB})^2}{(E_{ant})^2} = \frac{0.5 \times (25 \times 10^6)^2}{(500)^2} = 1.25 \text{ GW} \quad (2)$$

where E_{GB} represents waveguide breakdown field.

In SWA, high power handling sometime may require the holding of the antenna under vacuum or in a specific gas ambient such as SF_6 or N_2 to prevent early E-field breakdown or to improve the high power capacity of the system. For this purpose, SWA slots could be covered with an appropriate material such as a dielectric structure, which should maintain the radiation characteristics of the designed SWA array with improved high power handling capabilities. In this regard, a radome based on HDPE material ($\epsilon_r = 2.1$) was designed for the SWA array which could be employed either to create specific environment around the radiating array by injecting an appropriate gas or to create low pressure. The designed radome is shown in Fig. 13 along with its various dimensions. Figure 12(b) shows a variation in the electric field on the surface of the radome having its maximum value as 65 V/m, which leads to the power handling capacity, P_R, of the system as

$$P_R = \frac{P_{in}(E_{AB})^2}{(E_{ant})^2} = \frac{0.5 \times (3 \times 10^6)^2}{(65)^2} = 1.06 \text{ GW} \quad (3)$$

where E_{AB} represents air breakdown field.

III. FABRICATION, MEASUREMENTS AND DISCUSSION

A 50 mm thick aluminum slab was used for the fabrication of waveguide power divider and array antenna. The designed SWA was fabricated on the chosen aluminum slab by using milling and surface finishing tools of a multitasking MANDELLI machine. The complete model of the grooved SWAA system with and without radome is shown in Fig. 14. As explained before, the purpose of a radome is to keep the radiating waveguide under a controlled environment to manoeuvre the high power handling capacity of the system. The fabricated 1×4 waveguide based power divider along with 4-element based antenna is shown in Fig. 15. In this image, Fig. 15(a) shows the top view of the power divider whereas, its cut-view is shown in Fig. 15(b). The fabricated slotted waveguide having four elements separated by inside grooved is shown in Fig. 15(c). The antenna physical size in terms of wavelength ($\lambda_0 = 100$ mm) is $8.46\lambda_0 \times 4.3\lambda_0 \times 1.47\lambda_0$. An assembled SWAA by integrating all the parts explained in Fig. 15, is shown in Fig. 16, in an anechoic chamber for experimentation. In this figure, Fig. 16(a) shows

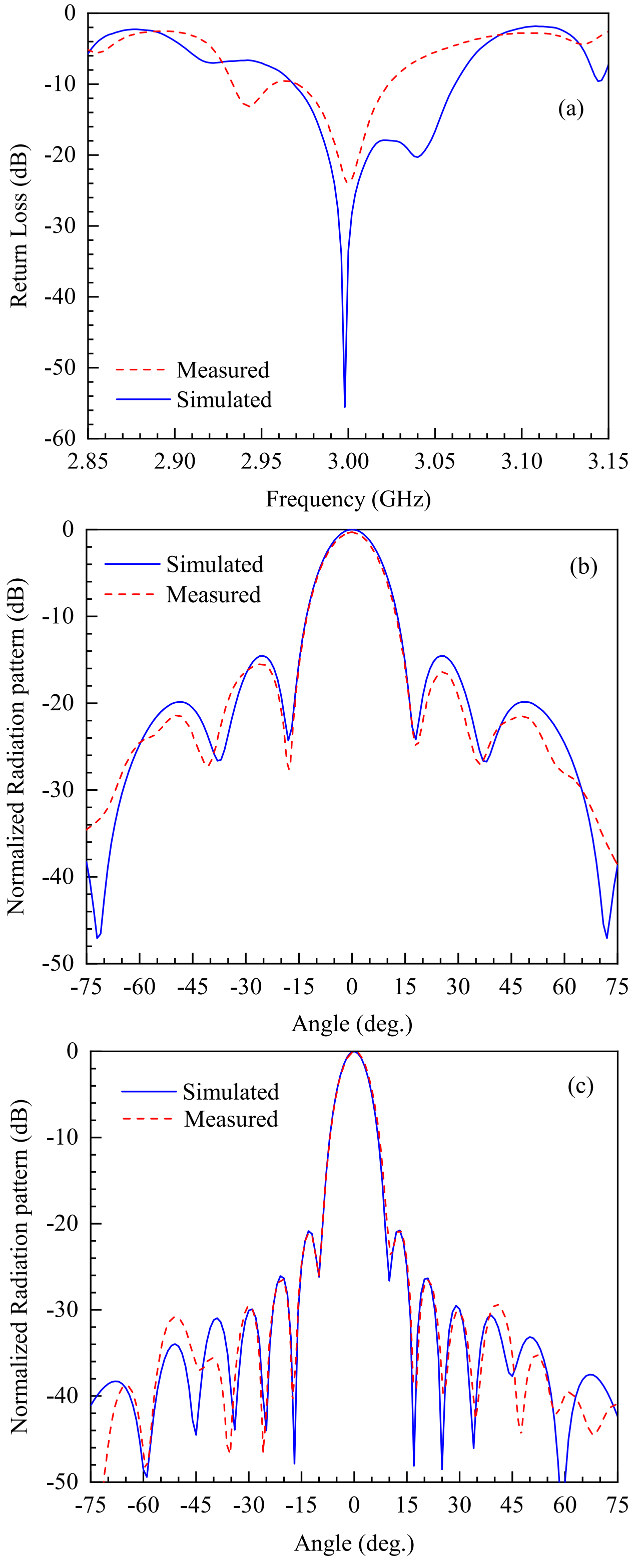

FIGURE 17. Measured and simulated radiation pattern of a 4-element slotted waveguide array antenna (without radome): (a) return loss, (b) E-field (c) H-field.

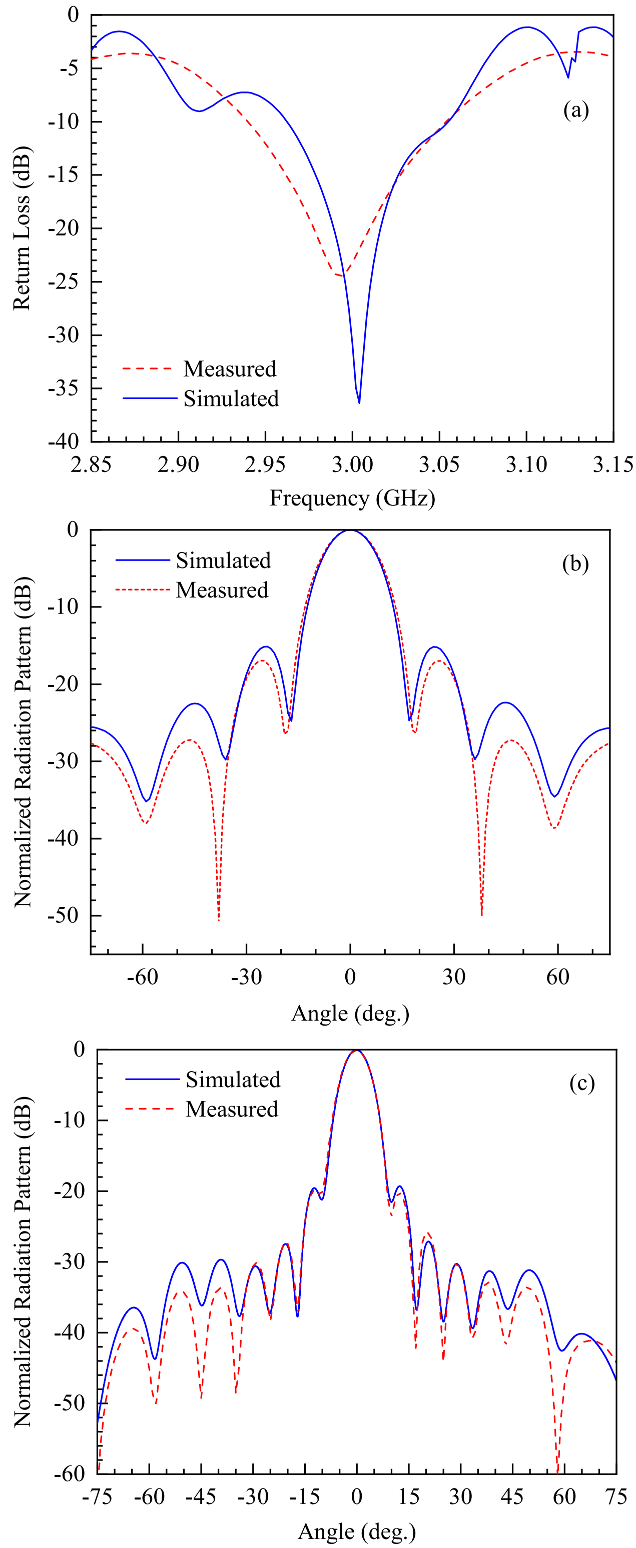

FIGURE 18. Measured and simulated response of a 4-element slotted waveguide array antenna with radome: (a) return loss, (b) E-field (c) H-field.

fabricated SWAA without radome whereas, Fig. 16(b) gives a pictorial view of fabricated SWAA with installed dielectric radome.

Rohde & Schwarz network analyzer, R&S ZNB20 was used to assess AC response of the array antenna. Near-field radiation pattern measurements were made using

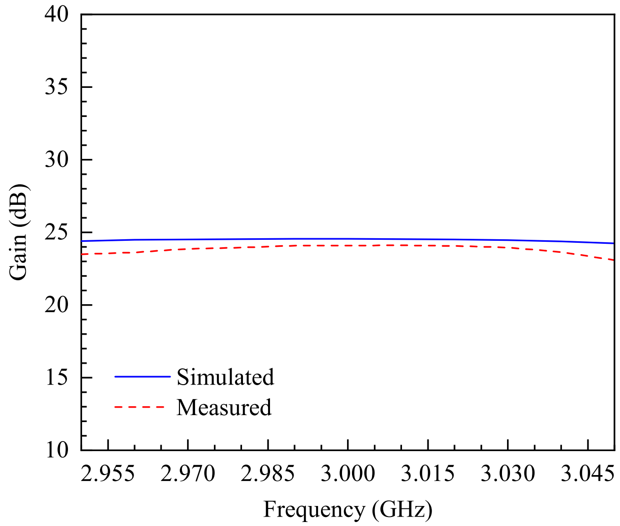

FIGURE 19. Observed and simulated gain of a 4-element slotted wave guide array antenna (SWAA) across its central frequency, f_0 =3 GHz.

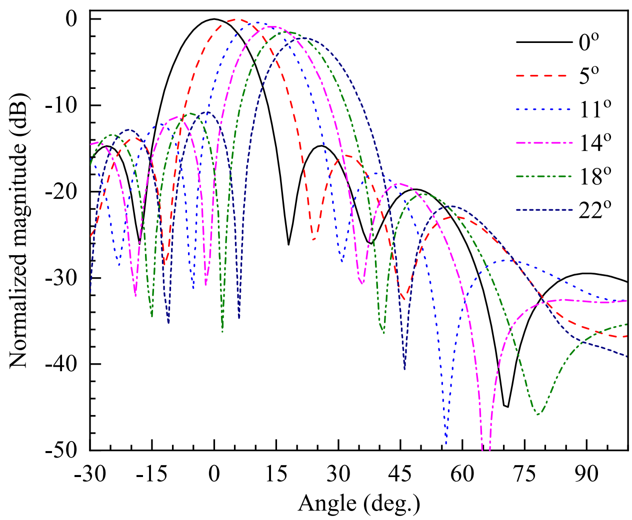

FIGURE 20. Measured beam steering results of a 4-element slotted waveguide array antenna (SWAA) system.

KEYCOM Model No. ANM01. Figure 17 shows measured and simulated RL, E-plane and H-plane responses of a fabricated 4-element array antenna (without radome). The plot of Fig. 17(a) exhibits that experimental data though show some deterioration in S_{11} characteristics but yet it maintains the magnitude of S_{11} below -20 dB at the central frequency for which it has been designed. The mismatch between simulated and observed characteristics could be associated to fabrication error tolerance and could be improved by improving fabrication technology. Plots of Fig. 17(b,c) also demonstrate that the simulated data is complying reasonably well with experimental measurements. Hence, this shows the proof of concept, and the proposed design can potentially be employed in HPM applications requiring GW energy.

On the other hand, Fig. 18 shows RL, electric and magnetic field radiation patterns of SWAA equipped with a dielectric radome as shown in Fig. 16(b). The plots of the figure once again demonstrate that SWAA with radome maintains system characteristics and the observed S_{11} magnitude is about -25 dB, which is better than the one observed in Fig. 17(a). However, in this case, a slight shift in the experimental peak relative to simulated data of S_{11} is noted, as shown in Fig. 18(a). The shift is minor and may not cause a significant change in the overall performance of the system. The main lobes both for E-and H-plane radiation patterns, as shown in Fig. 18(b,c), comply well with experimental characteristics. This shows that the ambient defined by the natural gases around the array can be further controlled to customize maximum power handling capacity of the system.

Experimental and simulated gain as a function of frequency is shown in Fig. 19. As ascertained before both simulated and observed characteristics are matching reasonably well and the system at its central frequency exhibits a gain of ∼25 dBi, which showed 7% improvement relative to Yong's design [9].

A comparison has been made between the preposed design and earlier similar published work by using central frequency f_0, size of the antenna, aperture efficiency, η, and the associated gain. The data in this respect is shown in Table 5. The magnitude of η is evaluated using [25]

$$\eta = \frac{\lambda^2 G}{4\pi S_A} \tag{4}$$

where G is the gain and S_A is the surface area of the antenna. Examining the data of Table 5, it can be seen that the proposed SWAA offers a competitive performance and could be a considered a potential design for HPM applications. The aperture efficiency of the proposed design is relatively better than the other designs listed in Table 5. This improved performance could be associated with the reduced MC values (-25 dB) due to optimally designed grooved structure on the broad-side walls of the waveguides.

The cold test of the array antenna beam steering measurements were performed using JFW Industry programmable phase shifter assembly 50PSA-102-06, and the measured steered beam patterns are shown in Fig. 20. By simultaneously observing the data of Fig. 11(a) and Fig. 20, one can comfortably conclude that the observed and simulated data are in good harmony, which demonstrates the proof of concept.

In order to perform a high power microwave test to analyze power handling capacity of the SWAA experimentally, a setup was developed as shown in Fig. 21. The SWAA was covered with the radome filled with SF_6. The relativistic magnetron was used to generate 1.2 GW pulses for an output frequency of 3.0 GHz with pulse repetition rate of 10 Hz. The directional coupler was used before the antenna array to measure the incident waveform. On the other hand, a detector

TABLE 5. Comparison of high power S-Band microwave antenna.

Ref.	f_0 (GHz)	Dimensions (mm^2)	Aperture efficiency (%)	SLL (dB)	Gain (dBi)	Power
Ref. [26]	3.17	416×34.04	50.25	-10	9.91	1.15 MW
Ref. [27]	3.15	1204×1215	43.5	–	27.70	500 kW
Ref. [28]	3.40	500×72	48.4	-15	14.5	–
Ref. [29]	2.40	350×740	60	-21	21.64	–
Ref. [30]	3.95	480×515	53.33	-22	24.60	6.25 MW
This work	3.00	846×430	63	-15	24.60	1.2 GW

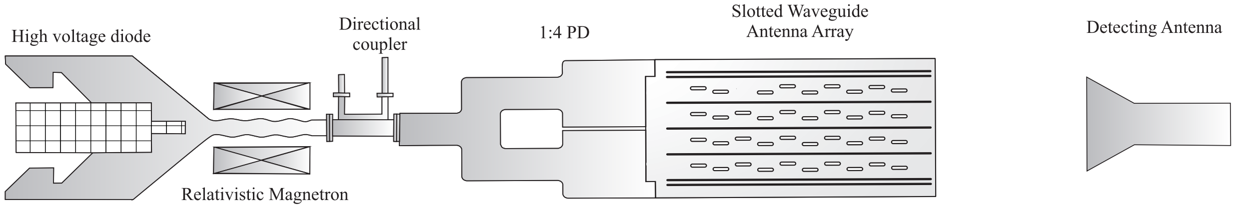

FIGURE 21. High power microwave test configuration of an array antenna.

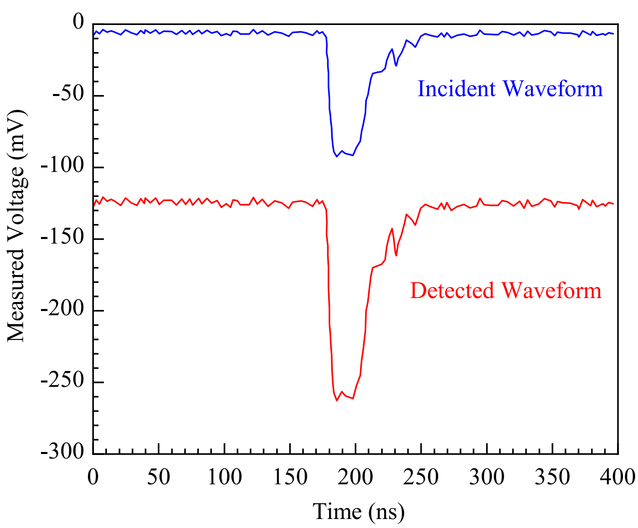

FIGURE 22. Incident and detected waveforms of an HPM test using the configuration shown in Fig. 21.

antenna was used to measure the radiated waveform in the far field region, as shown in Fig. 21. By examining the incident and the detected waveforms (Fig. 22), it can be concluded that there is no pulse shortening and that the two measured results had the same forms, which confirms that the system has the capacity to handle energy of at least 1.2 GW in S-band.

IV. CONCLUSION

In this manuscript, a slotted waveguide array antenna (SWAA) is developed for high-power microwave (HPM) applications in S-band. The array is developed by employing four slotted waveguide antenna of identical nature. The electromagnetic modeling was performed in CST MWS. The developed SWAA contained 4 elements, each has 10 rounded-edged leaky slots fabricated on the broad side-wall of an S-band waveguide. The array was designed at a central frequency of 3 GHz with power handling capacity greater than 1.0 GW. Slots of the array were distributed in a Gaussian profile to improve gain and to reduce side lobe levels (SLLs). In a four elements array each set of radiating slots are separated by a grooved line to reduce mutual coupling by controlling surface current. At the outer shoulder of the waveguide two additional grooves were fabricated to improve the radiation characteristics of the array. The designed SWAA was energized using a 1 × 4 power divider (PD) by ensuring equal power division with identical phase at each output port of the PD. To make the system robust and consistent, a dielectric radome is also designed and tested. A complete fabricated system is then characterized in an anechoic chamber with and without radome. The results so obtained were compared with the simulated data to demonstrate the validity of the design. Return loss of -25.5 dB at $f_0 = 3$ GHz is obtained when the system is measured without radome, whereas its value is -24.46 dB with radome. Experimentally, observed E and H planes radiation patterns showed a good degree of consistency with the simulated data. The fabricated system exhibited a gain of 24.11 dBi at 3.00 GHz whereas, the simulated data represented a gain of 24.55 dBi at 2.99 GHz. Additionally, SLL magnitude less than -20 dB in H-plane with no significant back and side lobes are observed. The developed technique exhibited a 7% increase in gain when compared with conventional (un-grooved) SWA. This enhancement in gain is associated with reduced mutual coupling using inside grooves and by employing Gaussian distribution in slots placement. The proposed technology exhibited a maximum of 33% reduction in mutual coupling in-between array elements when compared with the conventional design. The array provided $\pm 22^\circ$ beam steering with a nominal gain reduction of 2.2 dBi. The developed technique can be used in high-power microwave applications wherein its power handling capabilities can be adjusted as per the need of an application by inducing an appropriate ambient inside the radome.

REFERENCES

[1] R. J. Barker and E. Schamiloglu, *High-Power Microwave Sources and Technologies*. Hoboken, NJ, USA: Wiley-IEEE Press, 2001.

[2] J. Benford, J. A. Swegle, and E. Schamiloglu, *High Power Microwaves*. Boca Raton, FL, USA: CRC Press, 2015.

[3] G. A. Casula, G. Mazzarella, G. Montisci, and G. Muntoni, "A review on improved design techniques for high performance planar waveguide slot arrays," *Electronics*, vol. 10, no. 11, p. 1311, May 2021.

[4] L. Josefsson and S. R. Rengarajan, *Slotted Waveguide Array Antennas: Theory, Analysis and Design*. India: SciTech Publishing, 2018.

[5] Y. Tyagi, P. Mevada, S. Chakrabarty, and R. Jyoti, "High-efficiency broadband slotted waveguide array antenna," *IET Microw., Antennas Propag.*, vol. 11, no. 10, pp. 1401–1408, Aug. 2017.

[6] C. Chang, X. Zhu, G. Liu, J. Fang, R. Xiao, C. Chen, H. Shao, J. Li, H. Huang, Q. Zhang, and Z.-Q. Zhang, "Design and experiments of the GW high-power microwave feed horn," *Prog. Electromagn. Res.*, vol. 101, pp. 157–171, 2010.

[7] L. Guo, W. Huang, C. Chang, J. Li, Y. Liu, and R. Meng, "Studies of a leaky-wave phased array antenna for high-power microwave applications," *IEEE Trans. Plasma Sci.*, vol. 44, no. 10, pp. 2366–2375, Oct. 2016.

[8] Y. Yang, C. Yuan, and B. Qian, "A beam steering antenna for X-band high power applications," *AEU Int. J. Electron. Commun.*, vol. 68, no. 8, pp. 763–766, Aug. 2014.

[9] L. Yong, M. Fanbao, X. Gang, X. Ping, and M. Hongge, "Analysis of wide-angle scanning of HPM waveguide slot array antenna," *High Power Laser Beams*, vol. 30, no. 3, 2018, Art. no. 033002.

[10] L. Yu, C. Yuan, J. He, and Q. Zhang, "Beam steerable array antenna based on rectangular waveguide for high-power microwave applications," *IEEE Trans. Plasma Sci.*, vol. 47, no. 1, pp. 535–541, Jan. 2019.

[11] X.-Q. Li, Q.-X. Liu, J.-Q. Zhang, and L. Zhao, "16-element single-layer rectangular radial line helical array antenna for high-power applications," *IEEE Antennas Wireless Propag. Lett.*, vol. 9, pp. 708–711, 2010.

[12] B. El Jaafari and J.-M. Floch, "Gain enhancement of slot antenna using grooved structure and FSS layer," *Prog. Electromagn. Res. Lett.*, vol. 65, pp. 1–7, 2017.

[13] A. M. Khan, M. M. Ahmed, U. Rafique, A. Kiyani, and S. M. Abbas, "An efficient slotted waveguide antenna system integrated with inside-grooves and modified Gaussian slot distribution," *Electronics*, vol. 11, no. 18, p. 2948, Sep. 2022.

[14] M. Al-Husseini, A. El-Hajj, and K. Kabalan, "High-gain S-band slotted waveguide antenna arrays with elliptical slots and low sidelobe levels," *Prog. Electromagn. Res.*, vol. 1821, pp. 1–4, 2013.

[15] E. C. V. Boas, R. Mittra, and A. C. Sodre, "A low-profile high-gain slotted waveguide antenna array with grooved structures," *IEEE Antennas Wireless Propag. Lett.*, vol. 19, no. 12, pp. 2107–2111, Dec. 2020.

[16] C. Huang, Z. Zhao, Q. Feng, C. Wang, and X. Luo, "Grooves-assisted surface wave modulation in two-slot array for mutual coupling reduction and gain enhancement," *IEEE Antennas Wireless Propag. Lett.*, vol. 8, pp. 912–915, 2009.

[17] R. Meng, Y. Xia, Y. Guo, and Q. Zhu, "An X-band 48-way leaky waveguide antenna with high aperture efficiency and high power capacity," *IEEE Trans. Antennas Propag.*, vol. 66, no. 12, pp. 6799–6809, Dec. 2018.

[18] G. A. Deschamps, "Ray techniques in electromagnetics," *Proc. IEEE*, vol. 60, no. 9, pp. 1022–1035, Jun. 1972.

[19] S.-W. Lee, M. Sheshadri, V. Jamnejad, and R. Mittra, "Wave transmission through a spherical dielectric shell," *IEEE Trans. Antennas Propag.*, vol. AP-30, no. 3, pp. 373–380, May 1982.

[20] G. Montisci, Z. Jin, M. Li, H. Yang, G. A. Casula, G. Mazzarella, and A. Fanti, "Design of multilayer dielectric cover to enhance gain and efficiency of slot arrays," *Int. J. Antennas Propag.*, vol. 2013, pp. 1–6, Dec. 2013.

[21] T. Djerafi, A. Patrovsky, K. Wu, and S. O. Tatu, "Recombinant waveguide power divider," *IEEE Trans. Microw. Theory Techn.*, vol. 61, no. 11, pp. 3884–3891, Nov. 2013.

[22] R. Meng, H. Zhang, B. Muneer, and Q. Zhu, "The design of a 48-way high power capacity sectorial waveguide power divider," in *Proc. IEEE Antennas Propag. Soc. Int. Symp. (APSURSI)*, Jul. 2014, pp. 643–644.

[23] X. He, M. Hou, J.-R. Zhang, and Y.-L. Chi, "Development of four kinds of waveguide power divider for s band," 2016, *arXiv:1607.02816*.

[24] X. Zhao, C. Yuan, L. Liu, S. Peng, Q. Zhang, L. Yu, and Y. Sun, "All-metal beam steering lens antenna for high power microwave applications," *IEEE Trans. Antennas Propag.*, vol. 65, no. 12, pp. 7340–7344, Mar. 2017.

[25] Y. Wu, Z. Hao, Z. Miao, W. Hong, and J. Hong, "A 140 GHz high-efficiency slotted waveguide antenna using a low-loss feeding network," *IEEE Antennas Wireless Propag. Lett.*, vol. 19, no. 1, pp. 94–98, Jan. 2020.

[26] X. Pan, C. G. Christodoulou, J. Lawrance, J. McConaha, and M. Landavazo, "Cold & hot tests of an S-band antenna for high power microwave systems," in *Proc. IEEE Int. Symp. Antennas Propag. USNC/URSI Nat. Radio Sci. Meeting*, Jul. 2017, pp. 627–628.

[27] C. Martel, "A rectangular slotted waveguide array for high power microwave applications," in *Proc. IEEE Int. Symp. Antennas Propag. North Amer. Radio Sci. Meeting*, Jul. 2020, pp. 343–344.

[28] H. M. El Misilmani, M. Al-Husseini, and K. Y. Kabalan, "Design of slotted waveguide antennas with low sidelobes for high power microwave applications," *Prog. Electromagn. Res. C*, vol. 56, pp. 15–28, 2015.

[29] S. I. Alhuwaimel and K. Tong, "Stacked S-band slotted waveguide array antenna with very low sidelobes," in *Proc. Int. Workshop Electromagn., Appl. Student Innov. Competition*, May 2017, pp. 116–118.

[30] H. M. El Misilmani, M. Al-Husseini, and K. Y. Kabalan, "Design procedure for planar slotted waveguide antenna arrays with controllable sidelobe level ratio for high power microwave applications," *Eng. Rep.*, vol. 2, no. 10, p. 12255, Oct. 2020.

ASIF MEHMOOD KHAN received the M.Sc. degree in electronics from the University of Peshawar, Pakistan, in 1996, and the M.S. degree in electrical engineering from the Capital University of Science and Technology (CUST), Islamabad, in 2014, where he is currently pursuing the Ph.D. degree in high-power microwave antenna design. In 2015, he joined CUST as a Research Scholar. His research interests are high-power microwave generation, transmission, and their applications.

MUHAMMAD M. AHMED (Senior Member, IEEE) received the Ph.D. degree in microelectronics from the University of Cambridge, U.K., in 1995.

From 2007 to 2015, he was the Executive Vice President of Muhammad Ali Jinnah University, Karachi, Pakistan. He is currently the Vice Chancellor of the Capital University of Science and Technology. He developed a comprehensive framework to simulate and model electrical characterization of field effect millimeter wave transistors; both from analytical and numerical perspectives for improved understanding and CAD related applications. He also contributed in optimization of physical parameters of microwave field effect transistors for low noise applications. Through his sustained efforts, he developed and implemented a comprehensive strategy for university education and produced more than 11000 graduates at various levels to cater the needs of the society and to provide comfort to humanity. He supervised numerous M.S. and Ph.D. students in their research works. He has authored more than 160 research papers, published in journals of international repute. His research interests include RF engineering and microelectronics, specifically in microwave devices.

Dr. Ahmed was elected as a fellow of the Institution of Engineering and Technology (IET), U.K., in 1999. He was also awarded the title of Chartered Engineer (CEng) from the U.K. Engineering Council, in 1999, and a Gold Medal from the Pakistan Academy of Sciences for his outstanding contribution in the field of engineering and technology, in 2008. In 2002, he was honored with the title of Euro Engineer (Euro Ing) from the European Federation of National Engineering Association, Brussels. He has been the chair of a number of international conferences under the auspices of Institution of Electrical and Electronics Engineers (IEEE). He holds a life membership of IEEE Electron Devices, IEEE Microwave Theory and Technique, and IEEE Antenna and Wave Propagation Societies.

UMAIR RAFIQUE (Member, IEEE) received the B.S. degree in electrical engineering from Mohammad Ali Jinnah University (MAJU), Karachi, Pakistan, in 2011, and the M.S. degree in electrical engineering from the Capital University of Science and Technology (CUST), Islamabad, in 2017.

From June 2010 to January 2012, he was a Research Associate with the Research Group of Microelectronics, MAJU. From May 2013 to March 2015, he was an RF Design Engineer with AKSA Solutions Development Services (AKSA-SDS), where he was responsible for the design, development, and implementation of RF front ends for airborne and military applications. In October 2015, he joined the Microelectronics and RF Engineering Research Group, CUST, as a Research Associate, where he worked on numerous RF projects. He has published several research articles in reputed international journals and conferences and holds a research impact factor of more than 53. His research interests include MIMO antennas for sub-6 GHz and mm-wave applications, UWB and SWB antennas, lens antennas, frequency selective surfaces, metamaterials and meta surfaces, RF front ends and circuits, electronic system design and integration, and semiconductor device modeling.

Mr. Rafique is a member of the IEEE Antennas and Propagation Society (IEEE APS), USA, and the IEEE Microwave Theory and Techniques Society (IEEE MTTS), USA. He is a Registered Engineer with the Pakistan Engineering Council (PEC).

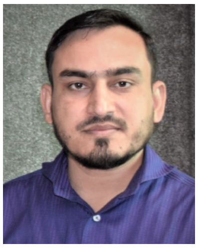

SULEMAN KHAN received the B.S. degree in electrical engineering from Mohammad Ali Jinnah University (MAJU), Karachi, Pakistan, in 2014, and the M.S. degree in electrical engineering from the Capital University of Science and Technology (CUST), Islamabad, in 2022. From 2015 to 2022, he was a Broadcast Engineer in campus radio with CUST. In 2023, he promoted as a Research Associate and joined the RF and Microelectronics Research Group, CUST, wherein he is involved in various research projects in the field of sensors, device modeling, and RF engineering. He is a Registered Engineer with the Pakistan Engineering Council (PEC).